

TENTATIVE APPRAISAL OF COMPATIBILITY OF SMALL-SCALE COSMIC MICROWAVE BACKGROUND ANISOTROPY DETECTIONS IN THE CONTEXT OF COBE-DMR-NORMALIZED OPEN AND FLAT- Λ COLD DARK MATTER COSMOLOGIES

KEN GANGA,¹ BHARAT RATRA,² AND NAOSHI SUGIYAMA³

Received 1995 December 29; accepted 1996 February 12

ABSTRACT

Goodness-of-fit statistics are used to quantitatively establish the compatibility of cosmic microwave background (CMB) anisotropy predictions in a wide range of Differential Microwave Radiometer (DMR) normalized, open and spatially flat Λ , cold dark matter cosmologies with the set of all presently available small-scale CMB anisotropy detection data. Conclusions regarding model viability depend sensitively on the prescription used to account for the 1σ uncertainty in the assumed value of the DMR normalization, except for low-density, $\Omega_0 \sim 0.3$ – 0.4 , open models, which are compatible with the data for all prescriptions used. While old, large baryon density, low-density, flat- Λ models ($t_0 \gtrsim 15$ – 16 Gyr, $\Omega_B \gtrsim 0.0175 h^{-2}$, $\Omega_0 \sim 0.2$ – 0.4) might be incompatible, no model is incompatible with the data for all prescriptions. In fact, some open models seem to fit the data better than should be expected, and this might be an indication that some error bars are mildly overconservative.

Subject headings: cosmic microwave background — cosmology: observations — large-scale structure of the universe

1. INTRODUCTION

Recent and near-future measurements of cosmic microwave background (CMB) anisotropy on a variety of angular scales, when used in conjunction with the predicted anisotropy in cosmogonical models, are in the process of transforming the CMB anisotropy field. Currently, one can only draw qualitative conclusions about the viability of broad-brush cosmological models, but it will soon be possible to set quantitative constraints on parameters of some specific models and to rule out other models. Until now all quantitative comparisons between model predictions and the data have made use of one of two simplifications: (1) data from one (or a few) experiments have been compared to predictions for one (or a class of) model(s), or (2) data from a larger number of experiments have been compared to predictions for a single model. While clearly a necessary first step, this approach has led to a number of vague claims about the (in)compatibility of some model(s) with some subset of the data, which, while perhaps correct, need to be put on firmer ground.

This work is a first attempt to compare all presently available CMB anisotropy detection data to predictions in a wide variety of observationally motivated cosmologies, with the ultimate goal of deciding, in a quantitative manner, whether any of these models are compatible with the wealth of CMB anisotropy data. Such a quantitative approach, using all available data, is essential if one wishes to draw robust conclusions about model viability. It will become more effective as the analyses are better understood and as the data improve. The only alternative is to wait a decade or so for a new CMB anisotropy satellite to address this issue.

To assess compatibility qualitatively, Ratra et al. (1995,

hereafter RBGS) and Ratra & Sugiyama (1995, hereafter RS) compared anisotropy predictions in 2 yr DMR-normalized, Gaussian, adiabatic, open and spatially flat Λ , cold dark matter (CDM) models (with the values of Ω_0 , h , and Ω_B chosen to satisfy non-CMB observational constraints,⁴ except in the fiducial CDM case) to small-scale anisotropy data.⁵ Here we use these predictions, in combination with a variety of goodness-of-fit statistics,⁶ to assess quantitatively the compatibility of CMB anisotropy detections. In contrast to RBGS and RS, we explore more options for accounting for the 1σ uncertainty in the DMR normalization, but in this preliminary analysis we ignore small-scale CMB anisotropy upper limits as well as the small correlations between data points from experiments with multiple windows (see § 3).

In a related analysis, Scott, Silk, & White (1995, hereafter SSW) used a Lorentzian approximation for the shape of the fiducial CDM model CMB anisotropy spectrum and concluded that it provided an adequate description of the anisotropy data (they took the data error bars to be symmetric). Here we use significantly more observational data, revised estimates of some of the older data (in general, newer results tend to be lower than older ones), and numerically computed CMB anisotropy spectra for a wider variety of models motivated by non-CMB observations. For all prescriptions we have used to account for the allowed 1σ range of the DMR

⁴ Low-density open and flat- Λ models are of current interest for a variety of observational reasons, including recent measurements that suggest a larger h , an older universe, and a smaller Ω_0 . Discussions of the observational motivation for the choice of cosmological parameters used here, as well as the non-CMB cosmological predictions of these models, may be found in RBGS, RS, and Ratra & Peebles (1994).

⁵ It is important to bear in mind that a variety of statistical techniques and prescriptions (as well as different assumed CMB anisotropy spectra) have been used to determine the observational results (RBGS); that the usual prescription for accounting for calibration uncertainty, by adding it in quadrature, is not quite correct (RBGS); and that non-CMB contamination and/or subtraction might be an issue in some cases.

⁶ We use various such statistics since most observational error bars are asymmetric (i.e., non-Gaussian).

¹ Division of Physics, Mathematics, and Astronomy, California Institute of Technology, Pasadena, CA 91125.

² Center for Theoretical Physics, Massachusetts Institute of Technology, Cambridge, MA 02139.

³ Department of Physics and Research Center for the Early Universe, University of Tokyo, Tokyo 113, Japan.

TABLE 1
NUMERICAL VALUES FOR MODEL PARAMETERS

Number	Ω_0	h	$\Omega_b h^2$
(O)0	0.1	0.75	0.0125
(O)1	0.2	0.65	0.0175
(O)2	0.2	0.70	0.0125
(O)3	0.2	0.75	0.0075
(O)4	0.3	0.60	0.0175
(O)5	0.3	0.65	0.0125
(O)6	0.3	0.70	0.0075
(O)7	0.4	0.60	0.0175
(O)8	0.4	0.65	0.0125
(O)9	0.4	0.70	0.0075
(O)10	0.5	0.55	0.0175
(O)11	0.5	0.60	0.0125
(O)12	0.5	0.65	0.0075
(O)13	1.0	0.50	0.0125
(A)14	0.1	0.90	0.0125
(A)15	0.2	0.70	0.0175
(A)16	0.2	0.75	0.0125
(A)17	0.2	0.80	0.0075
(A)18	0.3	0.60	0.0175
(A)19	0.3	0.65	0.0125
(A)20	0.3	0.70	0.0075
(A)21	0.4	0.55	0.0175
(A)22	0.4	0.60	0.0125
(A)23	0.4	0.65	0.0075
(A)24	0.5	0.60	0.0125
(A)25	1.0	0.50	0.0125

normalization, low-density open models with $\Omega_0 \sim 0.3$ – 0.4 are compatible with the data. Thus, we find that, consistent with the conclusion of SSW, a CMB anisotropy spectrum that mildly rises to multipole moments $l \sim 200$ is compatible with the data.⁷

2. SUMMARY OF COMPUTATION

We consider 32 smaller scale CMB anisotropy detections (almost entirely sensitive only to $l \lesssim 200$): FIRS (Ganga et al. 1994); Tenerife (Hancock et al. 1996); SK93, and individual-chop SK94 Ka and Q (Netterfield et al. 1996); SP94 Ka and Q (Gundersen et al. 1995); Python-G, -L, and -S (e.g., Platt et al. 1996); ARGO (de Bernardis et al. 1994); MAX3, individual-channel MAX4, and MAX5 (e.g., Tanaka et al. 1995); MSAM92 and MSAM94 (Cheng et al. 1996); and WDH1 (Griffin et al. 1996). For all detections (i), the observed band temperature, $\delta T_{(e)}^i$, and the 1σ upper and lower limits $\delta T_{(e)u}^i$ and $\delta T_{(e)l}^i$, are given in RBGS and RS (the subscript e denotes

⁷ As noted by SSW, such a rising CMB anisotropy spectrum is consistent with that expected from radiation pressure–induced oscillations at early times in the adiabatic structure-formation picture. It is also consistent with that expected in versions of the isocurvature scenario. There almost certainly are other models that are consistent with the data.

the experimental value). Also given there are 26 open and flat- Λ model predictions for the band temperature 1σ (Gaussian) upper and lower limits, $\delta T_{(m)u}^i$ and $\delta T_{(m)l}^i$ (the subscript m denotes the model prediction). The 1σ DMR range ($\sim \pm 11\%$) for the model predictions (derived from likelihood analyses of the DMR data using the model CMB spatial anisotropy spectra) accounts for statistical and systematic uncertainty in the DMR normalization (Stompor, Górski, & Banday 1995). (The DMR statistical uncertainty accounts for both intrinsic noise and cosmic variance.) The open-model predictions are given in RBGS (quadrupole-excluded, DMR–galactic-frame normalization), and the flat- Λ model predictions are given in RS (quadrupole-excluded, DMR–ecliptic-frame normalization).⁸ Further details may be found in these papers, while the model parameter values are listed in Table 1.

To assess the effect of varying the DMR normalization, we consider three sets of model predictions: one normalized to the lower 1σ DMR value, one normalized to the average of the upper and lower 1σ DMR values, and one normalized to the upper 1σ DMR value. We denote the model prediction for the i th detection $\delta T_{(m)c}^i$ (the central value of the model), and thus set it equal to $\delta T_{(m)l}^i$, $(\delta T_{(m)u}^i + \delta T_{(m)l}^i)/2$, or $\delta T_{(m)u}^i$ for the three prescriptions. For each of these predictions we also either include or ignore the model (i.e., DMR) “errors” $\sigma_{(m)}^i = (\delta T_{(m)u}^i - \delta T_{(m)l}^i)/2$, yielding six sets of predictions.

Five prescriptions, denoted I and outlined in Table 2, are used to construct the corresponding observational numbers for the small-scale anisotropy detections. The different prescriptions use different ways of estimating the “best” value for an experimental detection (either using the quoted detection value or an average of the upper and lower limits) and the error on the measurement (again using various combinations of the quoted limits).

For each model, model normalization, and model “error” prescription, and each detection i and data description prescription I , we define the quantity $D_{(I)}^i = (\delta T_{(e)c}^i - \delta T_{(m)c}^i)/\sigma^i$ as a measure of the deviation of the prediction from the observation. Here, σ^i is either $|\sigma_{(e)}^i|$ or $[(\sigma_{(e)}^i)^2 + (\sigma_{(m)}^i)^2]^{1/2}$. The $D_{(I)}^i$ are used to compute a reduced goodness-of-fit statistic, $\chi_{(I)}^2 = \sum_{i=1}^{32} (D_{(I)}^i)^2/32$ (the usual reduced χ^2 for points drawn from a Gaussian distribution). These are shown in Figures 1–6.

⁸ The ecliptic- and galactic-frame DMR maps are slightly different, and this is responsible for the small difference between the ecliptic- and galactic-frame normalizations (see, e.g., Bennett et al. 1996 and references therein). This difference is manifest in the results for models (O)13 and (A)25, which have identical CMB spatial anisotropy spectra, but are normalized using the different maps.

TABLE 2
PRESCRIPTIONS USED TO CONSTRUCT DETECTION NUMBERS

I	$\delta T_{(e)c}^i$	$\sigma_{(e)}^i$
1.....	$\delta T_{(e)}^i$	$\delta T_{(e)u}^i - \delta T_{(e)}^i$
2.....	$\delta T_{(e)}^i$	$(\delta T_{(e)u}^i - \delta T_{(e)l}^i)/2$
3.....	$(\delta T_{(e)u}^i + \delta T_{(e)l}^i)/2$	$(\delta T_{(e)u}^i - \delta T_{(e)l}^i)/2$
4.....	$\delta T_{(e)}^i$	$\begin{cases} \delta T_{(e)u}^i - \delta T_{(e)c}^i, & \text{if } \delta T_{(m)c}^i > \delta T_{(e)c}^i \\ \delta T_{(e)c}^i - \delta T_{(e)l}^i, & \text{if } \delta T_{(m)c}^i < \delta T_{(e)c}^i \end{cases}$
5.....	$\delta T_{(e)}^i$	$\delta T_{(e)}^i - \delta T_{(e)l}^i$

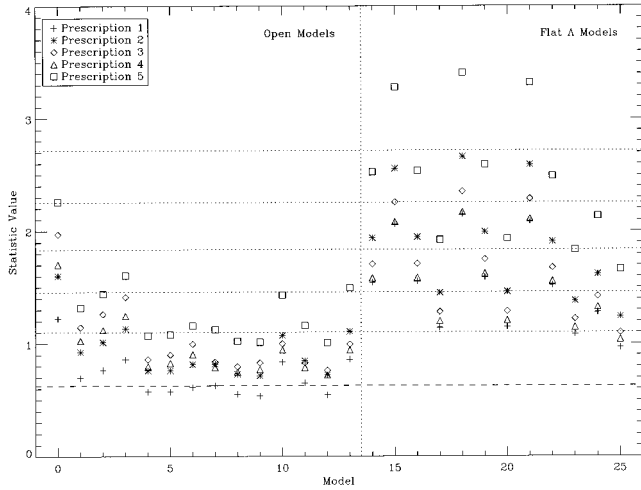


FIG. 1.—Five reduced (for 32 degrees of freedom) $\chi^2_{(l)}$, computed for the nominal value of the DMR normalization, and accounting for model “errors,” as a function of model number. The vertical short-dashed line divides the open models from the flat- Λ models. See Table 1 for model numbers and parameter values. The horizontal short-dashed lines are, in ascending order, at 1σ (31.7% probability of $\chi^2_{(l)}$ being this large or larger), 2σ (4.55% probability), 3σ (2.70×10^{-3} probability), 4σ (6.33×10^{-5} probability), and 5σ (5.73×10^{-7} probability) for 32 degrees of freedom drawn from a Gaussian distribution, and the horizontal long-dashed line is at the 95% probability level. Here, and in Figs. 2–6, the small differences between the $\chi^2_{(l)}$ values for the fiducial CDM models (O)13 and (A)25 (which have identical CMB spatial anisotropy spectral shape) are the consequence of the small difference between the DMR ecliptic- and galactic-frame normalizations.

3. DISCUSSION

Some of the 32 detections we use here are not completely independent. As a result, there are slightly less than the 32 degrees of freedom we have assumed. This causes our reduced $\chi^2_{(l)}$ values to be slightly smaller than they should be (a more accurate computation will require the appropriate correlation matrices). One might hope to compensate approximately for this by focusing on the $\chi^2_{(l)}$ computed using $D_{(l)}^i$ with $|\sigma_{(e)}^i|$ in the denominator instead of $[(\sigma_{(e)}^i)^2 + (\sigma_{(m)}^i)^2]^{1/2}$. This leads to $\chi^2_{(l)}$ values a bit larger than they should be, since it ignores

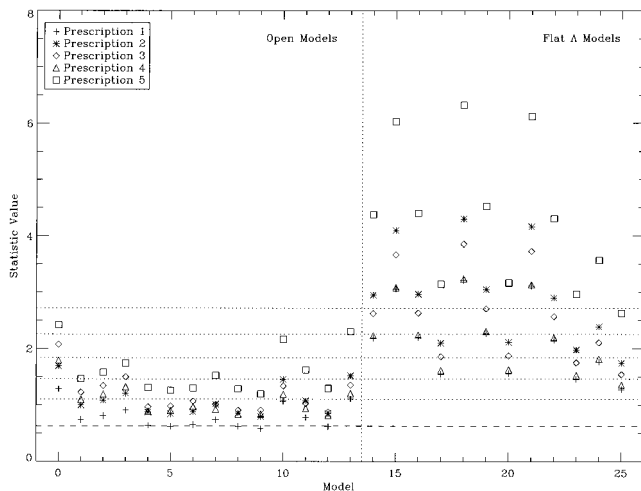


FIG. 2.—As for Fig. 1, but computed for the nominal value of the DMR normalization, and now ignoring model “errors.” Note that the vertical axis scale is different.

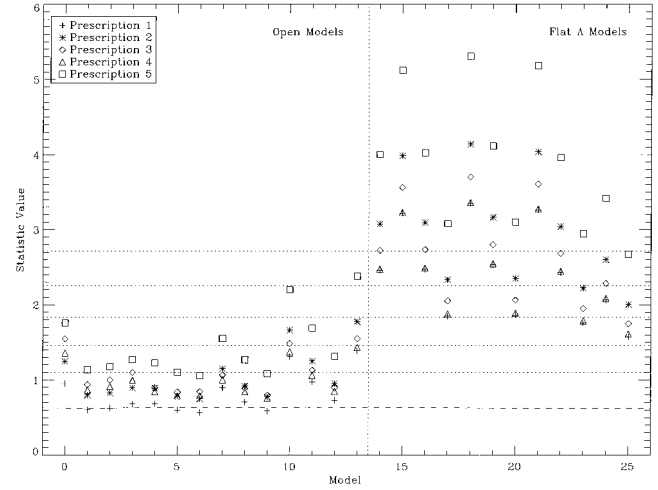


FIG. 3.—As for Fig. 1, but now computed for the upper 1σ value of the DMR normalization, and accounting for model “errors.” Note that the vertical axis scale is different.

the DMR noise uncertainty. Including both terms, however, leads to an overestimate of the uncertainty caused by cosmic variance, as this has already been accounted for in the small-scale data error bars, and exaggerates the uncertainty caused by systematic shifts in DMR normalization (which has already been accounted for by our use of three different DMR-normalization values).

The skewness and kurtosis of the 780 $D_{(l)}^i$ distributions for each model, DMR-normalization value, observational data prescription, and model “error” prescription are consistent with the range set by the variances of the skewness and kurtosis for 32 degrees of freedom drawn from a Gaussian distribution. This means that less compatible models (those with large $\chi^2_{(l)}$ in Figs. 1–6) are less compatible with the data because of many somewhat deviant predictions, and not because of just a few extremely deviant predictions.

First, we focus on the nominal DMR-normalized $\chi^2_{(l)}$ (Figs. 1 and 2), and we define a model as “compatible” with the data if $\chi^2_{(l)} < 1.46$, which marks the 2σ limit (4.55% probability of

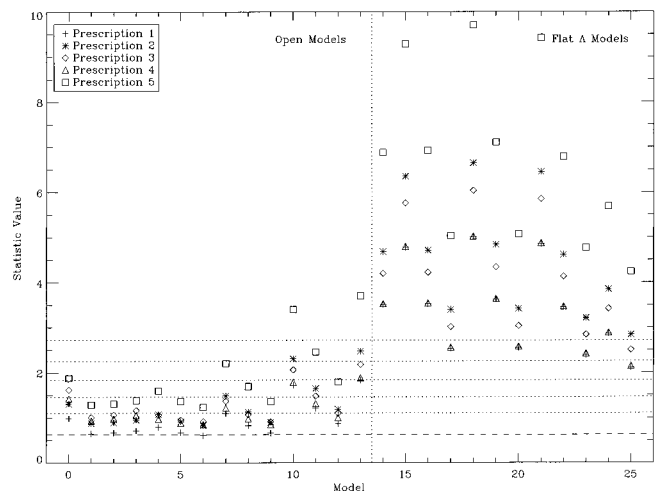


FIG. 4.—As for Fig. 1, but now computed for the upper 1σ value of the DMR normalization, and ignoring model “errors.” Note that the vertical axis scale is different.

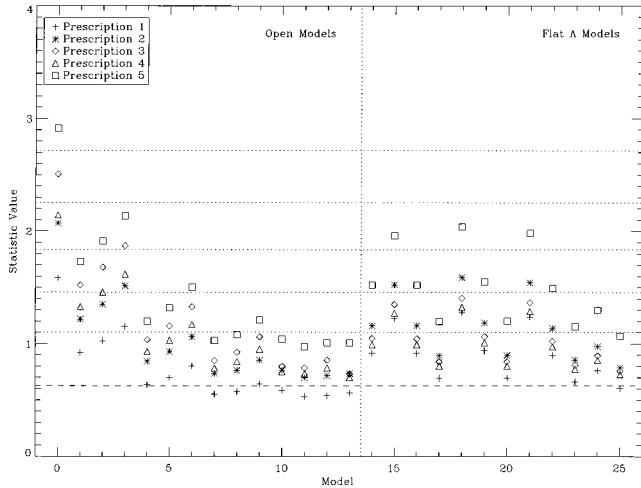


FIG. 5.—As for Fig. 1, but now computed for the lower 1σ value of the DMR normalization, and accounting for model “errors.”

$\chi^2_{(l)}$ being this large or larger) for 32 degrees of freedom drawn from a Gaussian distribution. Independent of the model “error” prescription, the only low-density ($\Omega_0 \sim 0.2\text{--}0.4$) flat- Λ models compatible with the data are the younger ($t_0 \sim 13$ Gyr), lower baryon density ($\Omega_B \lesssim 0.0075 h^{-2}$) ones,⁹ while all open models are compatible with the data (in agreement with the qualitative conclusions of RBGS and RS). For the upper 1σ value of the DMR normalization (Figs. 3 and 4), independent of the model “error” prescription, all flat- Λ models are incompatible, while low-density open models are compatible. At the lower 1σ value of the DMR normalization (Figs. 5 and 6), the $\Omega_0 = 0.1$ open model is incompatible, but most other models are compatible. In this case, conclusions regarding the viability of low-density ($\Omega_0 \sim 0.2\text{--}0.4$), old ($t_0 \sim 15\text{--}16$ Gyr), high baryon density ($\Omega_B \sim 0.0175 h^{-2}$), flat- Λ models depend sensitively on the model “error” prescription.¹⁰

Independent of the DMR-normalization value and model “error” prescription, low-density ($\Omega_0 \sim 0.3\text{--}0.4$) open models (models 4–9) are compatible with the data. This is our only robust conclusion about model viability. However, this is based

⁹ It might be significant that for flat- Λ models the CMB anisotropy data seem to favor a larger h and a smaller Ω_B , while some large-scale structure observations seem to favor a smaller h and a larger Ω_B (e.g., Stompor et al. 1995; SSW).

¹⁰ In our analysis, we have ignored upper limits. For the models we consider, the only seriously constraining upper limit is that of WDI (Tucker et al. 1993). This is mostly a serious constraint for the flat- Λ models (RS; RBGS), and is probably incompatible with these particular flat- Λ models (RS).

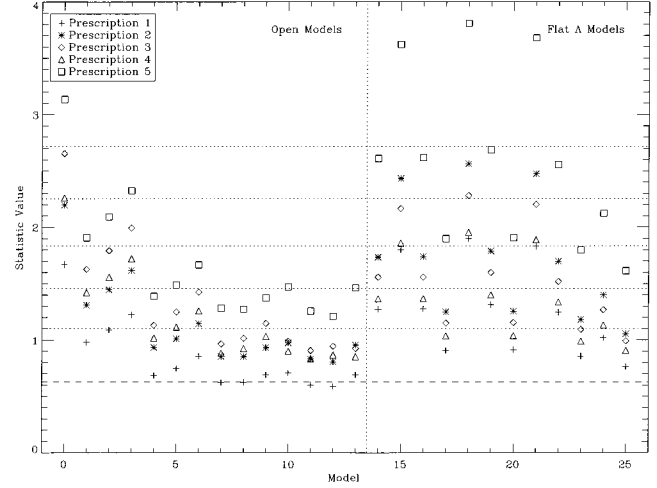


FIG. 6.—As for Fig. 1, but now computed for the lower 1σ value of the DMR normalization, and ignoring model “errors.”

on the assumption that there are no gross, unaccounted-for systematic uncertainties, and only means that, in this case, the quoted error bars are not unreasonably small. (We emphasize that even if there are gross, unaccounted-for systematic uncertainties, the CMB anisotropy detections could still be compatible, but with different models.)

A fairly large number of the $\chi^2_{(l)}$ are less than unity. While correlations between some data points certainly contribute to this, our understanding of the magnitude of the correlations leads us to suspect that mildly overconservative error bars on some of the data points might also be an issue. If this turns out to be more than just idle speculation, then, in combination with near-future improved small-scale CMB anisotropy data and the better normalization expected from the 4 yr DMR data,¹¹ our quantitative approach should allow for more robust conclusions about model viability.

We are indebted to T. Banday, L. Page, and J. Peebles, and also acknowledge useful discussions with E. Bertschinger, K. Górski, G. Griffin, J. Gundersen, B. Netterfield, U. Seljak, and S. Tanaka, as well as helpful comments from the referee.

¹¹ The new 4 yr DMR results (Bennett et al. 1996) indicate a normalization for power-law CMB spatial anisotropy models (Górski et al. 1996) that is slightly lower than that derived from the 2 yr DMR data. The open and flat- Λ models we consider here are not well approximated by power-law CMB spatial anisotropy spectra on the DMR scale, and the 4 yr DMR normalization of these models is not yet available. However, Figs. 1 and 2 correspond approximately to models that are normalized $\sim 2\sigma/3$ above the nominal value of the 4 yr DMR data, and Figs. 5 and 6 correspond approximately to models normalized $\sim 1\sigma/3$ below the nominal value of the 4 yr DMR data.

REFERENCES

- Bennett, C. L., et al. 1996, *ApJ*, submitted
 Cheng, E. S., et al. 1996, *ApJ*, 456, L71
 de Bernardis, P., et al. 1994, *ApJ*, 422, L33
 Ganga, K., Page, L., Cheng, E., & Meyer, S. 1994, *ApJ*, 432, L15
 Górski, K. M., et al. 1996, *ApJ*, submitted
 Griffin, G. S., Nguyen, H. T., Peterson, J. B., Tucker, G. S., & Dragovan, M. 1996, in preparation
 Gundersen, J. O., et al. 1995, *ApJ*, 443, L57
 Hancock, S., et al. 1996, in preparation
 Netterfield, C. B., Devlin, M. J., Jarosik, N., Page, L., & Wollack, E. J. 1996, *ApJ*, submitted
 Platt, S. R., Dragovan, M., Kovac, J., & Ruhl, J. E. 1996, in preparation
 Ratna, B., Banday, A. J., Górski, K. M., & Sugiyama, N. 1995, Princeton preprint PUPT-1558 (RBGS)
 Ratna, B., & Peebles, P. J. E. 1994, *ApJ*, 432, L5
 Ratra, B., & Sugiyama, N. 1995, Princeton preprint PUPT-1559 (RS)
 Scott, D., Silk, J., & White, M. 1995, *Science*, 268, 829 (SSW)
 Stompor, R., Górski, K. M., & Banday, A. J. 1995, *MNRAS*, 277, 1225
 Tanaka, S. T., et al. 1995, *ApJ*, submitted
 Tucker, G. S., Griffin, G. S., Nguyen, H. T., & Peterson, J. B. 1993, *ApJ*, 419, L45